PALACKÝ UNIVERSITY OLOMOUC

FACULTY OF SCIENCE

DEPARTMENT OF PHYSICAL CHEMISTRY

Adsorption of Biomolecules on Graphene and Fluorinated Graphenes

Bachelor Thesis

Author: Adam Matěj

Supervisor: Mgr. František Karlický, Ph.D.

Study program: B1407 Chemistry

Subject of study: 1407R023/00–1 Nanomaterial chemistry

Form of study: Full-time

Olomouc 2016

Declaration

I declare that I elaborated my bachelor's thesis independently under the guidance of Mgr. František Karlický, Ph.D. and all sources are included in the bibliography.

Olomouc:..... .....

Handwritten signature

Acknowledgement

I would like to thank my supervisor Mgr. František Karlický, Ph.D. for valuable advices, opportunities and patience in particular. I would also like to thank prof. RNDr. Michal Otyepka, Ph.D. for giving me chance to participate in this project.

Many thanks to my friends who were always supporting me and celebrating our successes together as well as those who kept pushing me forward even if they could not be with me.

Speciální poděkování patří mé rodině, která plně podporovala mé studium, věřili mým schopnostem a za to, že zůstali optimističtí i v posledních týdnech psaní této práce, kdy jsem je několik týdnů neviděl.

Bibliografické údaje

Autor: Adam Matěj
Název práce: Adsorpce biomolekul na grafenu a fluorovaných grafenech
Typ práce: Bakalářská
Vedoucí práce: Mgr. František Karlický, Ph.D.
Rok obhajoby: 2016
Pracoviště: Katedra fyzikální chemie, UP v Olomouci

Abstrakt: Tato práce se zabývá adsorpcí vybraných molekul na grafenu a jeho fluorovaných derivátech. Předmětem studia je jednak způsob adsorpce, a jednak vliv množství fluoru na adsorpční schopnosti. Výpočty byly provedeny za využití teorie funkcionály hustoty. Tři molekuly, NADH, dopamin, askorbová kyselina byly adsorbovány na grafen, fluorografen a dva částečně fluorované grafeny. Všechny molekuly vykazovaly stejný trend v adsorpci, tedy že nejméně vhodný povrch k adsorpci je fluorovaný grafen $CF_{0.25}$, zatímco nejlepší je slabě fluorovaný grafen s možností tvorby H-vazeb posílených π-π interakcemi. Druhý nejvhodnější je grafen využívající pouze stacking a následuje fluorografen. Využití adsorpce těchto molekul lze najít v konstrukci biosenzorů a detekrorů. Tyto senzory využívají velký povrch a vynikající elektrické vlastnosti 2D materiálů.

Klíčová slova: grafen, fluorografen, biosenzor, NADH, dopamin, askorbová kyselina, DFT
Počet stran: 35
Jazyk: Anglický

Bibliographic Identification

Author: Adam Matěj
Title: Adsorption of Biomolecules on Graphene and Fluorinated Graphenes
Type of thesis: Bachelor
Supervisor: Mgr. František Karlický, Ph.D.
The year of presentation: 2016
Department: Department of Physical Chemistry, UP Olomouc

Abstract: This thesis focuses on adsorption of selected molecules on graphene and its fluorinated derivatives. The subject of study is the way of adsorption, and the effect of amount of fluorine on the adsorption abilities. Calculations were performed using density functional theory. Three molecules, NADH, dopamine, ascorbic acid were adsorbed on graphene, fluorographene and two partially fluorinated graphenes. Each molecule showed the same trend in adsorption, so that the least suitable surface for adsorption is fluorinated graphene $CF_{0.25}$, while the most suitable is lowly fluorinated graphene with possibility to create H-bonds enhanced by π-π interactions. Second best suitable is graphene using only stacking interactions and fluorographene follows. Adsorption of these molecules can be used in construction of biosensors and detectors. These sensors use large surface area and outstanding electronic properties of 2D materials.

Keywords: graphene, fluorographene, biosenzor, NADH, dopamine, ascorbic acid, DFT
Number of Pages: 35
Language: English

Table of Contents

1. Introduction

The year 2004 was ground breaking for material sciences. As the first in the world, Geim and Novoselov isolated single layer of graphite. Atomically thin carbon sheet with hexagonal honeycomb lattice, nowadays known as graphene. Theoretically unstable carbon structure was proved to be stable in ambient conditions and following research showed graphene's unique properties.

Graphene sheet, although it is one atom thick, is mechanically very durable, has high transmittance and offers remarkable electronic properties. Besides its high thermal conductivity, electrical conductivity of graphene is caused by massless electrons moving near below the speed of light. This fact together with zero band gap electronic band structure with massless Dirac electrons makes graphene an excellent conductor and is referred to the thinnest known conductor. For its usage in electronics, it is necessary to open the band gap and transform excellent conductor into a semiconductor. This may be achieved amon others by covalent or noncovalent functionalization.

One possible way of usage is construction of detectors and biosensors using graphene derivatives as electrode surface. This thesis is a theoretical support for related experiment recently published in Nanoscale [1], where they constructed electrodes using differently fluorinated graphenes.

In this thesis was done the convergence study, geometry optimization of adsorbed molecules and adsorption energies calculations. To get the insight into adsorption on graphene derivatives, density functional theory corrected for description of London dispersion forces was used. All calculations were performed using Vienna Ab-initio Simulation Package.

2. Theoretical part

2.1. Graphene

Atomically thin carbon sheet with honeycomb lattice, a building material of graphite, that is carbon nanomaterial called graphene. First experimentally prepared strictly two-dimensional material which has been studied theoretically for many decades, nevertheless considered thermodynamically unstable. In 2004, Geim and Novoselov [2,3] managed to mechanically separate single layer of graphite and identify it by optical microscope. Optical methods were unable to use to identify atomically thin carbon sheets because of their high transmittance, but Geim and Novoselov discovered, that those sheets can be observable in visible spectra due to interfering Moiré patterns created on preferably thin (300 nm) silicon wafer [3]. This discovery began a new gold-rush in material sciences now interested in 2D materials. Besides fullerens and quantum dots from 0D family, nanotubes and needle-shaped nanomaterials from 1D branch, graphene and other later discovered 2D materials can find their usage in more daily-used applications. Thanks to the fact, that graphene creates sheets and due to its properties, there might be applications like displays construction, photovoltaic industry and many others branches using grapene's mechanical, optical and electronic properties.

2.1.1. Structural and electronic properties

As mentioned above, graphene is one sheet of graphite. Carbon atoms create planar honeycomb like structure with every atom in sp^2 hybridization with bond length of 1.425 Å. Since only one $2s$ with two $2p$ orbitals are hybridized, there is still one non hybridized $2p_z$ orbital. This orbital contents one electron and is perpendicular to the sheet, which allows it to interact with other non hybridized $2p_z$ orbitals. This way the π band is formed above and under the plane. Due to planarity, total conjugation of π electrons and satisfaction of Hückel's aromaticity rule, graphene is an aromatic molecule. As we know from chemistry of aromatics, it is most reactive towards the electrophilic substitution. Although sp^2 hybridization leads to planar structures, graphene sheet does not preserve its planarity at long ranges but creates waved structure instead. The disruption of planarity is caused by difference between the lattice constants of graphene and used base. With respect to the lattice differences

various Moiré patterns are formed [4–7]. Thanks to this effect it was possible to detect single-layer graphene using optical microscope despite the fact that single-layer graphene transmits over 95 % of light [8]. Even though graphene is only one atom thick it is hundreds of times stronger in tension than steel, flexible and chemically stable in ambient conditions.

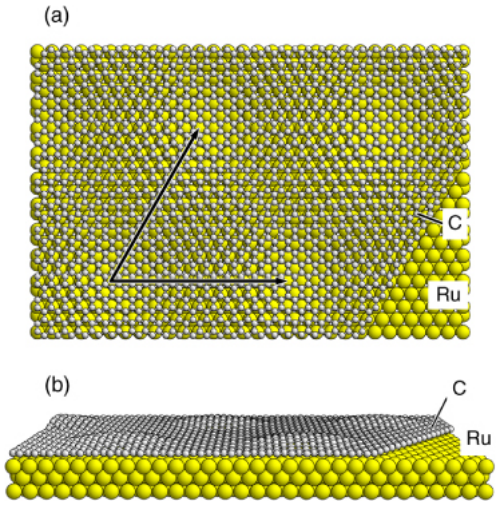

Figure 1: *Graphene overlayer adsorbed at the Ru(0001) surface. The Ru substrate surface is shown by its topmost three layers. (a) View perpendicular to the surface. The periodicity of the superlattice is indicated by arrows referring to Moiré lattice vectors. (b) View almost parallel to the surface, illustrating the periodic overlayer warping connected with the Moiré patterns shown in (a). Reprinted from [7].*

Not only has this novel material exceptional mechanical properties but reveals also new electronic features which come with its previously unattained dimensionality. Previous theoretical studies have already predicted some of those, for instance special electronic band structure and massless Dirac fermions. Electrons in graphene move at nearly speed of light (200 times lower than light of speed). This is because their transport is governed by Dirac's relativistic equation and they behave like particles with zero rest mass [9]. In solid state physics, allowed energies of electrons are described by the electronic band structure. Band structure of solids consists of three basic elements: valence bands, Fermi level and conductive bands. Valence bands form energetic continuum available for electrons in solid materials. Above the valence band there is Fermi level, characterizing material and structure as chemical potential. Fermi level is energy needed to add one electron to the structure. Third part of electronic band structure are conductive bands. Once again, it is a continuum of allowed energies for electrons, but unlike in the valence band, electrons

need additional energy for transition into conductive band. With this construction, three cases may appear.

The first possibility is that conductive band is connected with valence bands therefore electrons are able to travel freely throughout this material thus it is a conductor. Second case refers to semiconductors and insulators. When the conductive band is separated from the valence band, the band gap is created in between the two noted. Energetic values in band gap are forbidden for electrons hence frontiers of valence and conductive bands are created. The determination whether it is a semiconductor or insulator depends on the band gap value. In general, semiconductors usually have non-zero band gaps up to 2 eV. Electrons in these materials can be excited thermally, using gate voltage or by other methods depending on the material construction. Some semiconductors are using wider band gaps therefore the line between insulators and semiconductors is unclear. The third case is apparent as the borderline state between previous two cases. Zero-value band gap as special case will be discussed here for the reason that it occurs in graphene itself.

According to Bloch's theorem [10], periodic density can be described in periodic crystals using plane waves multiplied by periodic function. For easier computations it is convenient to use reciprocal space (k-space), so band structures are presented mostly in k-space over points with high symmetry - k-points. In periodical crystals, all calculations in reciprocal space are done in first Brillouin zone which contents different number of k-points. Brillouin zone is built same way as Wigner-Zeitz cell in real space. Special state occurs in graphene's band structure, which contains zero-value band gap. Conductive and valence bands are in contact at Dirac points (K and K' points) in first Brillouin zone with Fermi energy at this level. Graphene is a semiconductor without band gap, so at absolute zero and without structural disorders and impurities are all electrons in valence band. Technically no band gap allows electron excitations with ease in various energetic spectra. This may be caused thermally, applying gate voltage or using adsorbed molecules for structural disorders. Since conductive and valence bands are in contact, graphene is than a zero gap semimetal [11].

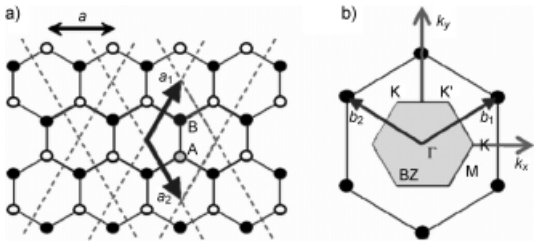

Figure 2: *a) Graphene lattice. a_1 and a_2 are the unit vectors. b) Reciprocal lattice of graphene. The shaded hexagon is the first Brillouin zone. b_1 and b_2 are reciprocal lattice vectors. Reprinted from [12].*

Due to the zero-value band gap, graphene shows great conductivity with high concentration of charge carriers and more interestingly, we can easily change the type of charge carriers [2]. This is achieved by electric field effect, which causes variations

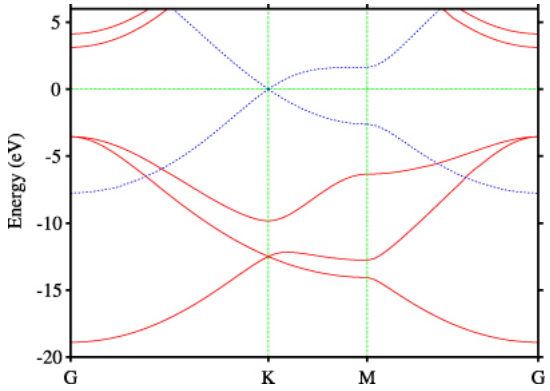

Figure 3: *Band structure of a single graphene layer. Solid red lines are σ bands and dotted blue lines are π bands. Reprinted from [13].*

in Fermi level depending on gate voltage applied. Both electrons and holes reach very high concentrations at wide temperature scale and without zero concentrations between this crossing. Electric field effect is very efficient in graphene sheets. This is because of the thickness that the field has to penetrate and it affects mostly the occupancy near the semiconductor surface. Therefore one can see that atomically thin layer with no band gap will be highly affected by the electric field. Engineers focused to create as thin semiconductor as possible using material compression but never achieved sheets thinner than hundreds of atoms. It was proved, that the concentration of charge carriers remains very high independently on temperature [9].

Graphene has high potential in electronics, but the key for the best possible use is to modify graphene's band structure and create desirable band gap. Pristine non-

disordered graphene lacks band gap, therefore some ways of modification come in mind. Easy way is to prepare graphene with structural disorders by preparation from graphene-oxide for instance. One of cons is that these impurities and structural imperfections are unable to be controlled [14, 15]. Other way to create band gap is to adsorb molecules and distort planarity. This method is easily controllable, but also has its cons. For instance very small gap opening and non-covalent interactions between surface and adsorbed molecules [16, 17]. Other non-covalent modification is possible by adsorption of more layers. The dependence of multiple layers on electronic properties has been studied as well, for example [18]. The structural modification is possible using so called doping, when carbon atoms are substituted with nitrogen or boron. The last way of gap opening mentioned here is covalent modification. Lot of studies have shown various ways of covalent derivation and their resulting effects. Very commonly used is halogenation [13, 19–22] and in this work I will focus especially on fluorination.

2.1.2. Applications

The enumeration of possible applications using graphene is so extensive [1,14,23–26], that I will present only some of the most interesting and the most promising applications depending on various properties. Many different studies of mechanical properties have shown extraordinary behaviour. Graphene has high potential in many constructions thanks to its highest tensile strength and durability of only one atomically thin sheet [27]. This fact together with high transmittance might help to find use in glass coverage and protection as well as ballistic protection. Not only is defect-free graphene more durable than kevlar, but also way lighter. For these purposes is the main problem preparation of larger sheets. The ability to resist strain altogether with uniquely high thermal conductivity and atomic dimensions makes graphene suitable and novel construction material in electronic circuits. Combination of great conductivity with transparency leads towards photovoltaic cells construction. For use in logic electronics it is necessary to open band gap and preserve great conductivity. Graphene based materials are meant to be perfect for energy storage applications for their thickness and very large surface area. Enormous surface area also offers possibility of electrochemical sensing.

2.1.3. Adsorption

Large surface area and electronic properties suitable for electrochemical sensing together with two-dimensional gas of π electrons predetermine graphene as material for construction of electrodes and biosensors. Many variations of construction were presented from pristine graphene and graphene oxide to chemically functionalized graphenes [25]. Graphene's planar structure with π electrons above the plane are accessible towards weak interactions using π-π interactions, the same forces that hold graphene sheets together in graphite. These so called stacking interactions are also engaged in adsorption of small aromatic molecules [28, 29]. The ratio of surface area / edge is so large, that only adsorption on surface plane is taken into account. On pristine graphene are available only interactions caused by London's dispersion due to lack of functional groups or other inhomogeneous sites for interactions.

2.2. Fluorinated graphene

This section is focused solely on fluorinated derivatives of graphene, their structure and differences in electronic properties against graphene's. Material scientists all over the world were and still are trying to tune band gap and other electronic properties by various functionalization approaches. Aforementioned path is covalent functionalization, especially fluorination. Few different derivatives are discussed here, therefore it is appropriate to clarify nomenclature used in this thesis. Fluorographene refers to fully fluorinated graphene with stoichiometry of C_1F_1 in each case. Other derivatives are reported as fluorinated graphenes or lowly fluorinated graphenes, with proper stoichiometries used as well.

2.2.1. Structural and electronic properties

On one side of the imaginary barricade is pristine graphene as an exceptional conductor, on the other side is one of the thinnest known insulators - fluorographene. Fluorographene surely brought new application possibilities by showing large band gap of 3.1[1] eV [30] or 3.8[2] eV [31]. Nevertheless theoretically calculated band gaps are in range 7-8 eV and 5-6 ev for electronic and optical band gaps respectively [21]. However, the goal is creation of band gap smaller than 2 eV and ability to tune this

[1] experimentally obtained optical band gap
[2] experimentally obtained electrical band gap including excitonic effects

value easily. This task is more complex, when we take into account the fact, that this new material has to have exceptional electronic properties to be advantageous. This includes high charge carrier mobility, stability in ambient conditions, durability, thermal conductivity and viable preparation. The reason I focus only on fluorinated graphenes, is that fluorination provides stable stoichiometries of CF_x where x is easily controlled and characterized. Various samples were theoretically studied and proved to have different direct and indirect band gaps in range from 0 to 8 eV [32].

Band gap differs with fluorine coverage and system of coverage, if fluorine atoms cover only one side or attach to surface from both sides. Due to disruption of sp^2 configuration, fluorine adsorb with respect to certain symmetries to minimize stress caused by neighbouring carbon atoms in sp^2 configuration. For example, very stable structures are $CF_{0.25}$ with one-side coverage and CF_1 with two-sides coverage. One-side coverage structure is most stable when F atoms are adsorbed around one benzene ring [33]. Other structures calculated in this work are proportionally similar to those experimentally prepared by Urbanova et al. [1] with stoichiometry adjusted to used supercells. Specific examples are described later in this work.

2.2.2. Adsorption

In the case of fluorinated graphene are interactions more complicated with respect to fluorine coverage and patterns created by adsorbed F atoms. It is clear, that in the case of CF the homogeneous π cloud above C atoms is absent due to sp^3 configuration and homogeneous band of partial negative charge is formed above very electronegative F atoms. If the amount of F atoms drops down, more C atoms in sp^2 configuration become accessible and depending on fluorination patterns [22] (one-side, two-sides, islands, armchair, zigzag, boat, chair) π-π stacking is available. High electronegativity of F atoms creates partial negative charges which can be involved in creation of hydrogen bonds with hydroxylic or amino groups of adsorbed molecules.

2.3. Selected molecules

2.3.1. NADH

First molecule, which attracted attention as substrate for detection using novel electrodes is nicotinamide adenine dinucleotide. Structure of NADH can be seen on fig. 4. This molecule occurs in two forms, oxidized and reduced, referred as NAD^+ and NADH respectively. This two electron reduction is very commonly used in enzymatic reactions where NAD^+ acts as coenzyme of oxidoreductases as oxidans. Similarly acts NADH in opposite reactions as reductans, which is source of electrons and hydrogen atoms. In human body joins NAD^+/NADH over 250 reactions. The reduction/oxidation happens on nicotine ring, where N atom is electron deficit in oxidized form. By accepting one H^+ and two electrons transforms nicotine ring in reduced form with reorganization of π bonds and transforming C atom in *para* position according to N atom into sp^3 configuration. Adenine is aromatic as well as nicotinamide in oxidized form. This allows stronger interactions with surface due to conjugated π electrons above and under the ring. Reduced form contains only one aromatic ring the form of adenine. The reduction of nicotinamide disrupts aromaticity, thus NADH is less stable and oxidation is endergonic reaction. Detection of NAD^+/NADH is key for study of lactate dehydrogenase, strong adsorption of NADH on surface without its reduction is wanted in possible use in energy storage devices [1, 34].

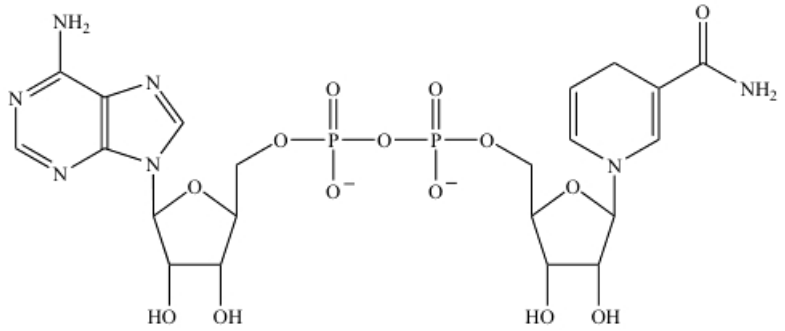

Figure 4: *Nicotinamide adenine dinucleotide.*

2.3.2. Ascorbic acid

Ascorbic acid (AA), vitamin C, is very important antioxidant in biochemistry thanks to easy dehydrogenation and formation of dehydroascorbic acid (fig. 5). Ascorbic

acid is able to undergo one- or two-electron reduction important in neutralization of free radicals in organism. In human body takes AA place as coenzyme, antioxidant and supports immune system. AA often interferes in detection DA [25], therefore its characterization is needed. The fact that ascorbic acid is not aromatic suggests weaker interactions also due to only small ring according to NAD^+ two aromatic rings.

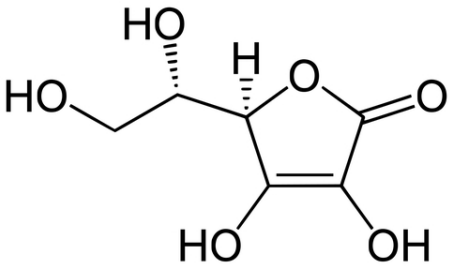

Figure 5: *Ascorbic acid.*

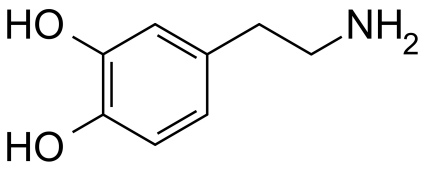

Figure 6: *Dopamine.*

2.3.3. Dopamine

Third studied molecule is dopamine (DA), well known neurotransmitter whose low level causes Parkinson's disease and high levels cause schizophrenia. Accurate, fast and stable methods of detection are requested for determination of DA levels in patients with Parkinson's disease because DA and other antiparkinsonics (DA precursors) are given to patients as treatment. Dopamine satisfies conditions of aromaticity, hence DA's aromatic ring can again interact with graphene using stacking.

2.4. Quantum mechanics

The 20^{th} century witnessed great discovery, when Austrian physicist Erwin Schrödinger invented non-relativistic stationary mathematical equation predicting wave functions, that can describe particles state and properties. He formulated time-independent Schrödinger equation

$$\widehat{H}\psi = E\psi, \tag{1}$$

where ψ is wave function, $\widehat{H}$ is Hamiltonian and E is energy of the system. Numerical solution gives us more solutions for energy from which the lowest is the ground state. To be able to calculate the ground state numerically, we need to know the form of $\widehat{H}$, which consists of kinetic energy and potential energy. Here the problem

becomes more complex in systems with more particles and we introduce useful approximations. First approximation neglects influence of electron movement to nuclei (proton is 1800 times heavier than electron), so that the kinetic energy of nuclei is not included. We say that nuclei are stationary in space and this approximation is called Born-Oppenheimer approximation.

$$(\widehat{T}_e + \widehat{V}_{NN} + \widehat{V}_{Ne} + \widehat{V}_{ee})\psi_e = E_e\psi_e \tag{2}$$

In this state we have simplified equation, but as we can see in equation 2, besides the kinetic energy of electrons we have also nuclei-electron and electron-electron interactions noted as $\widehat{V}_{Ne}$ and $\widehat{V}_{ee}$ respectively. $\widehat{V}_{NN}$ is potential of nucleus-nucleus interaction and is equal to constant in Born-Oppenheimer's approximation. The last variable becomes numerically very complicated when we analyse system with more electrons. Total electronic wave function can be approximately described as a product of wave functions of individual electrons. Total wave function can be obtained by calculating Slater determinant with one-electron wave functions which can be constructed using known functions. This known set of functions is called basis set (of plane waves or gaussians etc.) and we specify them in particular computations.

Wave function as such is not measurable and useful is only its square $|\psi|^2$ which evaluates the probability of occurrence in space. All electrons are equal and we are unable to say, which electron will be on which place in space, but we can say, that an electron will be in this place (more accurately volume in space) with certain probability. Electron density gives us the information about the probability of electron existence in an infinitesimal volume of space. The equation of electron density can be constructed using one-electron wave functions approximation

$$\rho(\overrightarrow{r}) = 2\Sigma_i\psi_i^*(\overrightarrow{r})\psi_i(\overrightarrow{r}), \tag{3}$$

here ρ is an electron density obtained from summation of complex conjugation of one-electron wave functions. Two electrons cannot have the same set of quantum numbers. They can have the same three quantum numbers describing the quantum state, but they have to differ in spin. The multiplication by two in equation 3 is for two electrons with different spin.

2.5. Density functional theory - DFT

According to Hohenberg-Kohn's theorem from 1964, we can get the wave function and therefore the ground state from the electron density. The first theorem states, that "*the external potential* $V_{ext}(\overrightarrow{r})$ *is (to within a constant) a unique functional of* $\rho(\overrightarrow{r})$*; since, in turn* $V_{ext}(\overrightarrow{r})$ *fixes* $\widehat{H}$ *we see that the full many particle ground state is a unique functional of* $\rho(\overrightarrow{r})$". Thus we are able to describe energy of the system if we know the electron density of this system

$$E_0[\rho_0] = T[\rho_0] + E_{Ne}[\rho_0] + E_{ee}[\rho_0]. \tag{4}$$

If we rewrite equation 4 to separate system dependent and independent variables we get

$$E_0[\rho_0] = \int \rho_0(\overrightarrow{r}) V_{Ne} d\overrightarrow{r} + T[\rho_0] + E_{ee}[\rho_0], \tag{5}$$

where the integral is system dependent and terms behind integral are independent. Now we can rewrite independent variables into more convenient form

$$E_0[\rho_0] = \int \rho_0(\overrightarrow{r}) V_{Ne} d\overrightarrow{r} + F_{HK}[\rho_0], \tag{6}$$

in which the $F_{HK}[\rho_0]$ is called the Hohenberg-Kohn functional. The $F_{HK}[\rho_0]$ is independent on system, hence it can be used on every system calculated, but we do not know its real form [35].

The second Hohenberg-Kohn theorem is based on variational principle and says, that the ground state density determines the lowest energy and any other density results in energy higher than the ground state energy. By using trial density in equation 6 we get ψ and therefore energy of the system. This calculated energy is upper bound to the true ground state. Calculated energy belongs to the ground state energy if and only if the density of the ground state is used. We do not know the true form of $F_{HK}[\rho_0]$ and therefore we are unable to find the ground state by changing only the density.

To be able to vary $F_{HK}[\rho_0]$ it is necessary to separate this functional into known parts, from which we do not know the exchange-correlation functional. In 1965 pre-

sented Kohn and Sham mathematical apparatus for calculating the ground state energy. They suggested a way to find potential needed in calculating one-electron wave functions by iterative calculating of this potential using trial density. Kohn-Sham's equations are constructed as bellow

$$\left(-\frac{1}{2}\nabla^2 + \left[\int \frac{\rho(\overrightarrow{r}_2)}{r_{12}} + V_{XC}(\overrightarrow{r_1}) - \sum_A^M \frac{Z_A}{r_{1A}}\right]\right)\psi_i = \left(-\frac{1}{2}\nabla^2 + V_S(\overrightarrow{r}_1)\right)\psi_i = \epsilon_i\psi_i \tag{7}$$

$$V_S(\overrightarrow{r}_1) = \int \frac{\rho(\overrightarrow{r}_2)}{r_{12}} d\overrightarrow{r}_2 + V_{XC}(\overrightarrow{r}_1) - \sum_A^M \frac{Z_A}{r_{1A}} \tag{8}$$

The key problem here is the term V_{XC} which is the exchange-correlation potential [36].

For sufficient and accurate solutions the correct form of V_{XC} is needed, thus this is the key problem of DFT calculations using Kohn-Sham's relations. Since we are unable to predict proper form of the exchange-correlation functional, we are again forced to use various approximations. Here I will talk about two functionals used in this study, especially Perdew-Burke-Ernzerhof (PBE) [37] functional using generalized gradient approximation (GGA) and with empirical dispersion correction (PBE-D2). Second functional used is optB86b-vdW.

Firstly mentioned PBE functional uses GGA, which calculates V_{XC} as interactions between electron and local density gradient computed as first derivation of density. Its accuracy and distance of counted density is maintained by cut-off, but it does not describe weak interactions on longer distances. Therefore empirical dispersion correction is used in PBE-D2 functional, which can be described as semiempirical method. Simple addition of $\frac{C}{r^6}$ is added to result from PBE functional [38]. This additional term is as simple as could be, because C is a constant characterising interaction between two certain atoms and r is distance between these two atoms. Second used density functional optB86b-vdW is optimized version of van der Waals density functional (vdW-DF) counting weak interactions on long distances in principle [39]. Functionals from vdW-DF family are still not quite correct because of the form of functional describing long distance densities and different functionals are needed for different systems. Due to more complicated functional structure use of vdW-DF is

computationally more expensive for larger systems. As mentioned before, we do not know the exact form of exchange-correlation functional, thus different systems have to be calculated using different functionals developed and parametrized for similar systems.

Now it is convenient to remind the Bloch's theorem and plane waves when solving problems in crystals. Due to infinite periodicity in crystals (without defects) we can simplify our calculations using reciprocal space (k-space) in which we are able to describe wave function as product of plane wave and periodical function, which has the same period as the lattice. Plane waves are periodical and infinite, as well as crystal structure. It is impossible to calculate with infinity, thus we specify certain energy cut-off and only plane waves with kinetic energy lower or equal to this cut-off value will be calculated. This set of plane waves create the basis set. Reciprocal space is constructed as Fourier transformation from real space, thus the k-space has its own structure and symmetry. As we built Wigner-Seitz cell in real space, we can use same technique to create first Brillouin zone. In calculations, the Brillouin zone contains high-symmetry points in which is the Schrödinger's equation calculated. We are also unable to form infinite crystal structure so the feature of periodic boundary conditions implemented in program mentioned later.

In Vienna Ab-initio Simulation Package (VASP) program which I was using for all calculations the cut-off energy is specified by variable called encut and it is set in eV. Another parameter important for accurate calculations is the number of k-points over which is the Schrödinger's equation calculated. Number of k-points and mesh over first Brillouin zone is specified in a input file called kpoints. Together with file incar, which contains various parameters, forms the base of technical specification for each calculation. Yet another files are needed to start the job, poscar file contains coordinates of each atom in the cell, vectors and lattice constants to form the cell. Fourth necessary file is potcar in which are pseudopotentials for each atom in system.

3. Practical part

3.1. Vienna ab-initio simulation package

All calculations were carried out using Vienna Ab-initio Simulation Package (VASP) for DFT calculations in crystals. This program has its convenient features for simplifying studies of periodical systems. The main feature for crystals is periodical boundary conditions. This means that we create a unit cell which has all properties of the whole crystal (symmetry, lattice constant, elements) and then every other cell is image of this model cell. Therefore if one atom leaves the cell on one side, it appears back from the other side, thus the number of atoms is preserved. How to create the unit cell? The smallest possible cell which has all periodical properties of crystal is called elemental cell. From this cell we can create the crystal by copying the elemental cell using translational vectors.

Second simplification is due to implemented PAW (projector augmented wave) method [40], which uses differently constructed pseudopotentials. The difference from former pseudopotentials is in the description of inner electrons and core, which together form potential interacting with valence electrons. Pseudopotentials for each element of studied system are located in potcar file, which is one of four necessary input files for calculations.

Other three input files are incar, kpoints and poscar. Poscar contains translational vectors, lattice constant and coordinates of each atom. Kpoints file, as name suggests, specifies number and mesh of k-points in first Brillouin zone. Incar file is technically the most complex, because lots of parameters are set here. One of them is aforementioned encut variable. Other variables define e.g whether the job is done in real or reciprocal space, maximal number of electronic steps, maximal number of geometrical steps, energy criteria for iterations, number of bands in electronic band structure and lots of others.

3.2. Convergence study

It is necessary to set parameters for calculation right to get reliable results. Since technical demands differ task to task, the proper way to get the needed set-up is

to work out the convergence study. By systematically changing variables we get different results with certain errors which are decreasing in the case of convergence. Then we decide which setting to use according to required error.

All calculations for convergence study were performed on system DA on pristine graphene using PBE-D2 functional. Structures of adsorbed DA on surface were obtained by systematic geometry optimization calculations where parameters were gradually tightened after successful optimization on previous set-up. This procedure allowed faster geometry optimization. Studied parameters were encut and prec, where latter specifies precision used in calculation (besides encut specifies also grid for fast Fourier transformation).

The studied property was adsorption energy E_{ad} obtained as difference in energies between adsorbed molecule and free molecule and graphene

$$E_{ad} = E_{mol+sur} - E_{mol} - E_{sur}, \tag{9}$$

where E_{mol} and E_{sur} are total energies of free[3] molecule and free surface respectively.

The INCAR file used in this study is changing only in encut and precision values with other parameters set as follows: Ispin=1; Ediff=1E-05; Lvdw=.true.; Lreal=auto. This set-up says, that calculation was carried out in real space counting with van der Waals interactions (PBE-D2), with closed shell (non spin polarized) and that optimization was finished when change in energy was less than 0.0001 eV from last electronic step.

3.3. Studied systems

Fluorinated graphenes in experiment [1] were prepared with stoichiometries as follows: $F_{0.084}$, $CF_{0.158}$, $CF_{0.218}$. In my work I studied two boundary cases, pristine graphene and fluorographene. Besides these two structures I used two lowly fluorinated graphenes as well. Due to different dimensions of chosen molecules, supercell had to be proportional to these molecules.

[3]Placed alone in enough large cell to avoid interactions between its copies, simulating vacuum.

Molecule of NADH is 22.2 Å long, therefore larger supercell had to be used. Two boundary cases were pristine graphene and fluorographene, both with 338 C atoms in supercell constructed as 13 × 13 unit cells. The same size was used for special stoichiometry of $CF_{0.0059}$ ($C_{338}F_2$) on which I tested possible hydrogen bonds. Very stable structure creates fluorinated graphene with stoichiometry of $CF_{0.25}$ with two-side coverage. This cell has different unit cell, therefore 12 × 12 supercell ($C_{288}F_{72}$) was created. Cells had to be of these dimensions, so there would not be interactions between molecules in neighbour cells.

Dopamine and ascorbic acid are about same size, 8.6 Å and 7.1 Å respectively, so the same cell was used for both molecules. Here pristine graphene, fluorographene and lowly fluorinated graphene $CF_{0.02}$ ($C_{98}F_2$) used 7 × 7 supercell with 98 C atoms. As well as for NADH, $CF_{0.25}$ was created, here with 4 × 4 supercell ($C_{128}F_{32}$).

Structural properties vary with level of fluorine coverage. Bond length in graphene is 1.425 Å with lattice constant 2.468 Å. Bond lengths in fluorographene are 1.58 Å and 1.38 Å for C-C and C-F respectively, with lattice constant of 2.607 Å. In $CF_{0.25}$, C-F length is increased to 1.48 Å with lattice constant of 4.98 Å. Two different C-C lengths are present. Between two nonfluorinated C atoms the bond length is 1.401 Å and 1.503 Å between one fluorinated and one nonfluorinated C atom. C-F length in the lowest fluorine coverage (two F atoms per cell) is 1.46 Å. Due to the dimensions of supercells, all NADH calculations were carried out using 1 × 1 × 1 k-points, while DA and AA were calculated using 2 × 2 × 1 k-points, both Brillouin zones were Γ-centred.

3.4. Geometry optimization

All calculations on non-optimized systems of adsorbed molecules on surfaces were performed by systematic tightening of conditions. Structures were prepared by placing the molecule above the surface in the distance of 3 Å with aromatic rings parallel to the surface. In the case of NADH, two possibilities were studied. First the NADH in its native geometry was placed over the surface, where neither adenine or nicotine (non-aromatic in NADH) were parallel to the surface. Thus I changed the geometry

of NADH using GaussView 5 program to create structure, where both rings are in one plane. The geometry first mentioned has shown not to be as profitable as the second one (on all surfaces), thus only the second one is discussed in this thesis.

As the adsorbed system was prepared, calculations were started using low encut (350 for NADH and 400 for DA and AA), ediffg (energy difference between geometry steps) was set to 1E-02 and ediff (energy difference between electronic steps) was set to 1E-03. Geometry optimization was performed in real space on low or normal precision (NADH or DA/AA respectively). After satisfying criteria of geometry optimization (ediffg) the parameters were tightened to encut=300 and prec=normal. First optimizations were also carried out using fixed surface atoms, so only relaxation of molecule was done. This allowed faster progress. Tightening was continued to encut=450, prec=accurate.

When the system has been optimized, parameters from convergence study were applied to obtain representative absolute energies for PBE-D2 and optB86b-vdW. From these calculations I received adsorption energy E_{ad} from equation 9. Here the free surface and free molecule (using the same cell size) energies were obtained by applying the same parameters.

4. Results and discussion

4.1. Convergence of energy

Convergence study was performed on encut values from 300 eV to 550 eV with steps of 50 eV using three precisions (low, normal, accurate). Figure 7 shows evolution of E_{ad} obtained by PBE-D2. It is clear that using cut-off 500 eV with accurate precision causes strange behaviour. After checking if all input files are all right, the only possible reason to this behaviour came to my mind. Lreal tag parameter changes four parameters with encut among others. Then the sampling of the grid for fast Fourier transformation (FFT) is varied automatically depending on encut specified in the incar file. Thus I tried to calculate the values for encut=450-550 on accurate precision using lreal=false, which calculates in reciprocal space. After that I fitted obtained values into previous graph which can be seen in figure 8.

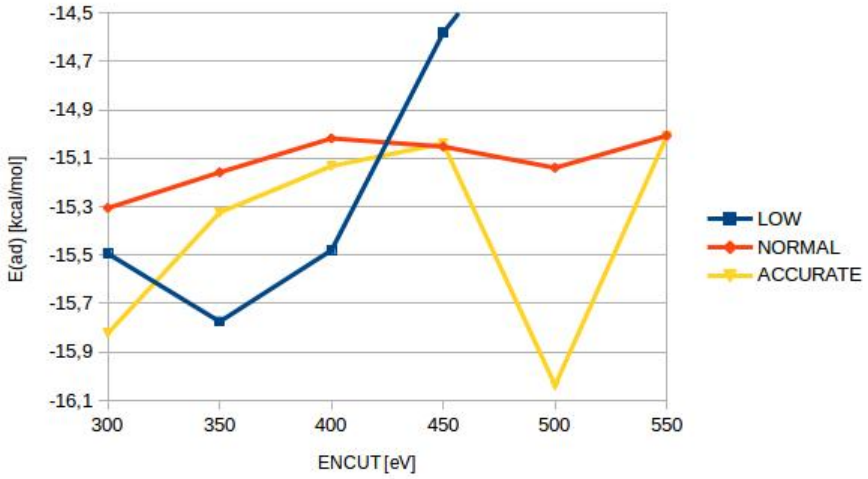

Figure 7: *Original convergence study using PBE-D2 functional on system DA on graphene. Value for cut-off 500 eV on accurate precision is most likely cause by automatically sampled grid for FFT.*

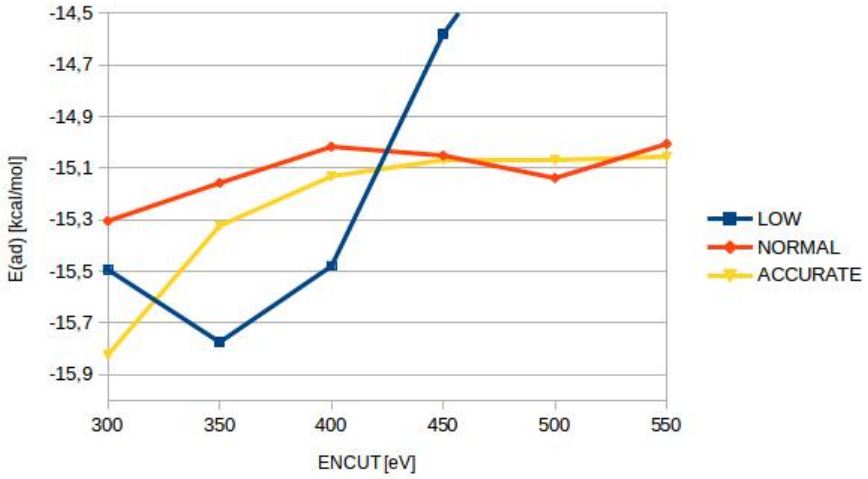

Figure 8: *Convergence study with fitted part of cut-off 450-550 eV obtained from calculations in reciprocal space using lreal=false.*

It is obvious that second graph with fitted part (encut 450-550 with lreal=false) does not show any strange behaviour. Optical evaluation is inadequate, therefore relative errors were calculated and obtained values are shown in table 1. Precision low does no converge in tried range of cut-off energy and relative errors only confirm this fact. When using normal precision, the convergence curve is not consistent and errors vary too much in tested range. The accurate precision on the other hand

shows clean convergence curve (with fit) and after 450 eV cut-off the percentage errors are smaller than 0.5 %.

Table 1: *Relative errors of second (fitted) convergence, values in %. Relative error was calculated according to equation 10.*

	Encut [eV]				
	350	400	450	500	550
Low	1.78	1.91	6.17	4.21	18.41
Normal	0.97	0.94	0.23	0.58	0.88
Accurate	3.26	1.27	0.42	0.01	0.09

$$\delta x = \frac{x_{i-1} - x_i}{x_i}, \tag{10}$$

here x_i is actual value and x_{i-1} is previous value. After this convergence study and appropriate relative errors I have considered to use 450 eV cut-off energy with accurate precision for single-point total energy calculations.

4.2. Adsorption energy

Each molecule successfully adsorbed on every surface and all cases showed negative E_{ad}, which indicates that attractive forces are stronger than repulsive forces (total energy is more negative). Table 2 summarizes adsorption energies of all systems and one can see that the order of suitable surfaces is the same for all three molecules. This points to the same way of interaction. It is clear that the best surface

Table 2: *Adsorption energies calculated using optB86b-vdW [kcal/mol].*

Surface \ Molecule	**NADH**	**DA**	**AA**
Graphene	-67.6	-21.7	-22.3
Fluorographene	-43.7	-17.9	-17.5
$CF_{0.25}$	-38.5	-11.0	-10.2
$CF_{0.0059}$ / $CF_{0.02}$	-72.9	-26.8	-25.5

for adsorption of these molecules is fluorinated graphene with low level of fluorine coverage. The reason of this behaviour can be better understood by focusing on the effect of fluorine presence for adsorption. If we take a look at figure 9 then we can see that in all three cases the molecule arranges its OH group towards the F atom, which is reminds the formation of hydrogen bond. Visual similarity with H-bond is

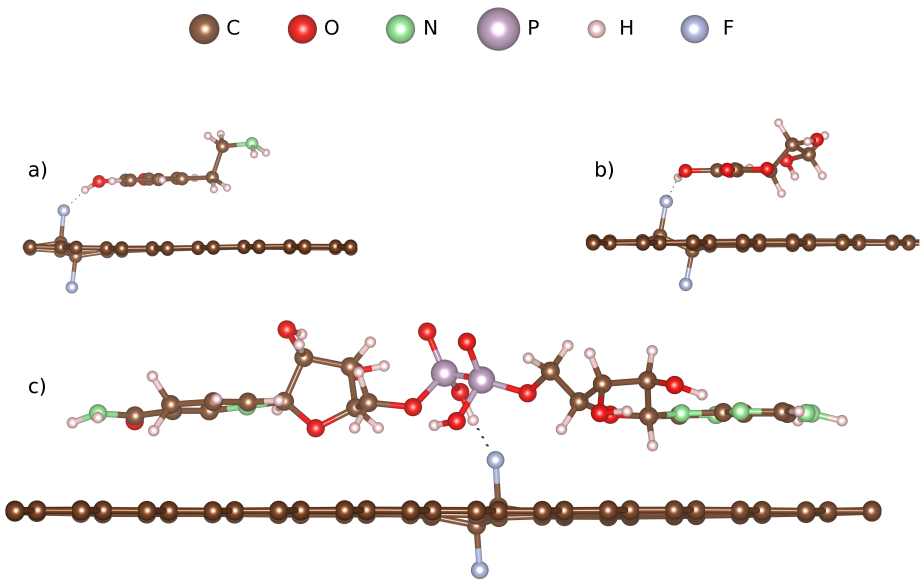

Figure 9: *Each molecule forms hydrogen bond between OH group and F atom on surface. It is also clear that each molecule preserves parallel with surface. a) dopamine b) ascorbic acid c) NADH*

not enough, therefore detailed structural parameters are included in table 3. Second

Table 3: *Bond lengths (Å) and hydrogen bond angle for each molecule on lowly fluorinated graphene. O-H refers do bond length between oxygen and hydrogen in hydroxylic group. H$\cdots$F refers to distance between fluorine and hydrogen from hydroxylic group. Third column contains angles between three aforementioned atoms.*

Molecule \ Bond	**O-H**	**H$\cdots$F**	**$\angle$O-H$\cdots$F**
NADH	1.00	1.56	167.0 °
Ascorbic acid	0.98	1.86	163.9 °
Dopamine	0.98	1.74	169.9 °

most advantageous surface is pristine graphene. It is obvious after looking at figure 10, because we can see the same stacking interaction as in the case of low fluorinated graphene with the difference, that no H-bonds are created here.

To describe this stacking interaction more, I measured distances of each molecule to the surface. In order to obtain representative data, I proceeded as follows: position of molecule was established as average z position of atoms forming main ring. In the case of NADH the average was calculated from both adenine and nicotine together. Similarly the surface z position was averaged. Obtained distances are summarised in table 4.

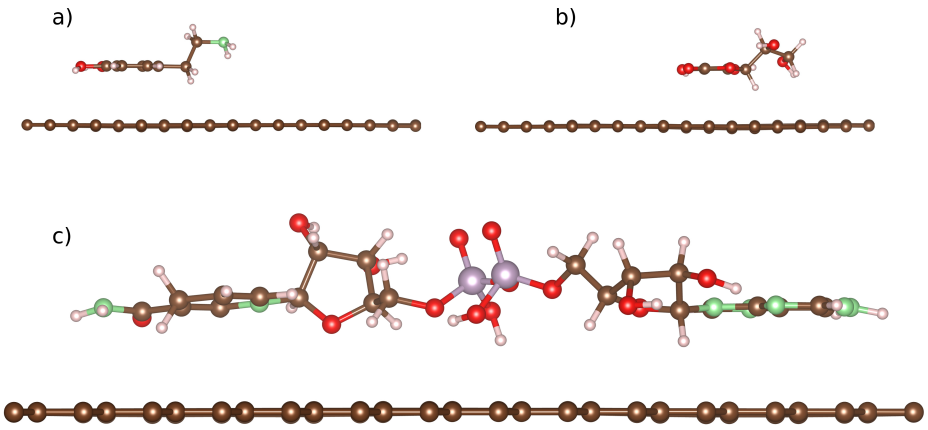

Figure 10: *Conformation of molecules on pristine graphene. a) dopamine b) ascorbic acid c) NADH. The rings of all molecules are parallel to graphene plane.*

Table 4: *Distances [Å] between adsorbed molecules and surfaces are given here. In cases where two numbers are given, the first refers to distance to C atoms, whereas second refers to distance to F atoms*

Surface\Molecule	**NADH**	**DA**	**AA**
Graphene	3.06	3.21	3.11
Fluorographene	4.24 / 2.84	4.33 / 2.95	4.26 / 2.88
$CF_{0.25}$	4.21 / 2.42	4.66 / 2.88	4.55 / 2.76
$CF_{0.0059}$ / $CF_{0.02}$	3.28	3.19	3.11

Concerning interaction strength, after graphene follows fluorographene and partially fluorinated graphene ($CF_{0.25}$) respectively. On these surfaces are molecules adsorbed the weakest and it is caused by the structurally hindered graphene islands for stacking in $CF_{0.25}$ and totally absent C atoms in sp^2 configuration. As we can see, molecules are attracted to fluorographene stronger than to partially fluorinated graphene. This is caused by homogeneous and more compact layer of fluorine atoms with partial negative charge. This creates high electron density which can interact with molecule by London's dispersion. In the case of $CF_{0.25}$ with two-side homogeneous coverage, fluorine atoms are too spread (two nearest F atoms are distanced 4.98 Å). Figures 11 and 12 show adsorbed molecules on CF and $CF_{0.25}$.

According to experiments in [1], my findings about adsorption on fluorinated gra-

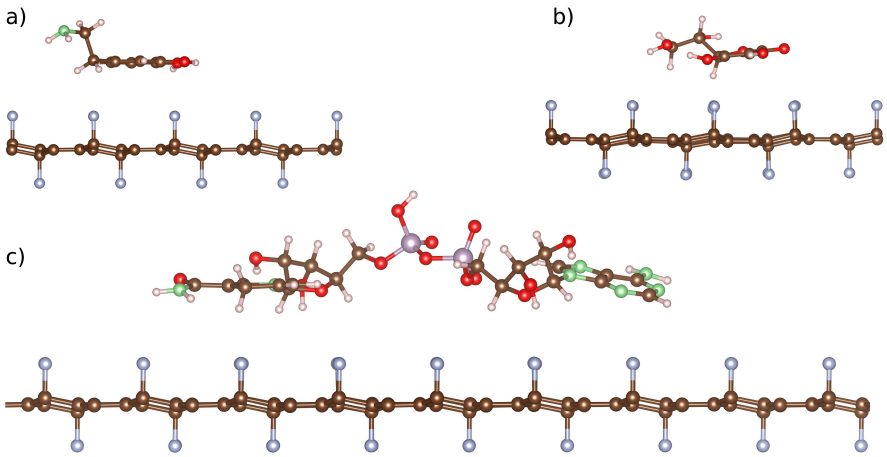

Figure 11: *Molecules adsorbed on surface of $CF_{0.25}$. It is visible that adenine ring of NADH is slightly turned around and does not preserve geometry parallel with surface. The same effect is remarkable in the case of ascorbic acid. This fact might be responsible for lower adsorption energies on $CF_{0.25}$.*

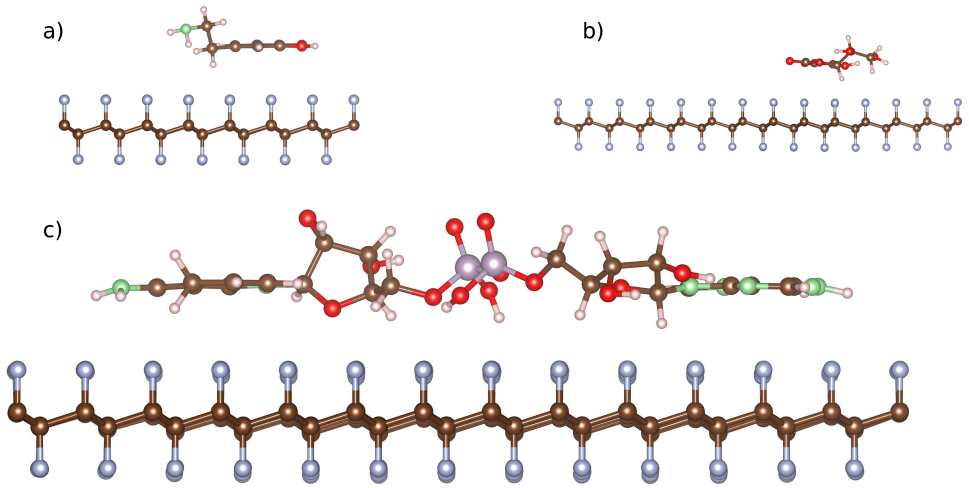

Figure 12: *Molecules adsorbed on surface of CF. In comparison with figure 11, all rings stay parallel to surface, which gains higher adsorption energies.*

phenes are in agreement with electron transfer in certain surfaces. Data included in my thesis therefore supports experiment sufficiently.

5. Conclusion

The aim of my thesis was to study the effect of fluorine on adsorption on differently fluorinated graphenes. Three molecules, namely nicotinamide adenine dinucleotide, dopamine and ascorbic acid, were adsorbed on pristine graphene and three differently fluorinated graphenes. I was using density functional theory as implemented in Vienna Ab-initio Simulation Package (VASP).

On pristine graphene was the adsorption caused by π-π stacking, when all three molecules tended to place their rings (heterocycles, aromatic rings) parallel to the graphene's plane. Each molecule was optimized in the distance slightly over 3 Å from graphene, which is typical value for van der Waals interactions. Graphene was used as reference surface.

Second reference surface was fluorographene as the second extreme due to maximal possible fluorine coverage. All molecules adsorbed on fluorographene relatively strongly due to homogeneous layer of fluorine atoms with partial negative charge on them.

Fluorinated graphene with low level of coverage, the case when there were only two fluorine atoms per cell, was the third surface studied. This system was constructed hence formation of hydrogen bonds was expected. The formation of hydrogen bonds was proved in all three molecules. Due to large area of sp^2 carbon atoms there was possible adsorption by stacking enhanced by H-bonds. Therefore is graphene with low degree of fluorination perfect for adsorption of similar molecules.

The last surface studied was partially fluorinated graphene with very stable stoichiometry and structure. $CF_{0.25}$ with homogeneous two-side coverage is the worst surface for adsorption studied in this thesis. Due to the ratio of sp^2 C atoms and

F atoms, stacking is not sterically available and due to low amount of F atoms the interaction with homogeneous layer is also not available.

This thesis covers the theoretical background for related experiment, yet still offers space for further study. One possibility is to study the influence of adsorption onto band structure.

6. Závěr

Cílem mé práce byla studie vlivu přítomnosti a množství fluoru na adsorpci na různě fluorované grafeny. Tři molekuly, přesněji nikotinamid adenin dinukleotid, dopamin a kyselina askorbová, byly adsorbovány na čistý grafen a tři různě fluorované grafeny. Používal jsem teorii funkcionálu hustoty, zahrnutou v programu VASP.

Na čistém grafenu byla adsorpce způsobena π-π stackingem, kdy všechny tři molekuly měly své cykly paralelně s rovinou grafenu. Každá molekula se optimalizovala do vzdálenosti okolo 3 Å od grafenu, což je typická vzdálenost pro van der Waalsovy interakce. Grafen byl použit jako referenční povrch.

Druhým referenčním povrchem byl fluorografen jako druhý extrém díky maximálnímu možnému pokrytí fluorem. Všechny molekuly se na fluorografen adsorbovaly realtivně silně díky homogenní vrstvě atomů fluoru s částečným záporným nábojem.

Fluorovaný grafen s nízkým stupněm pokrytí, ten případ, kdy v buňce byly pouze dva atomy fluoru, byl třetí studovaný povrch. Tento systém byl vytvořen jako předpoklad pro možnou tvorbu vodíkových vazeb. Tvorba vodíkových vazeb byla dokázána u všech tří molekul. Díky velké oblasti s uhlíky v sp^2 konfiguraci byl možný stacking posílený vodíkovými vazbami. Proto je slabě fluorovaný grafen nejvhodnější povrch pro adsorpci podobných molekul.

Poslední studovaný povrch byl částečně fluorovaný grafen s velmi stabilní stechiometrií a strukturou. $CF_{0.25}$ s homogenním oboustraným pokrytím je ze zkoumaných povrchů ten nejméně vhodný pro adsorpci. Kvůli poměru sp^2 uhlíků a atomů fluoru, není možný stacking ani interakce s homogenní vrstvou atomů fluoru.

Tato práce zajišťuje teoretickou podporu pro související experiment, ale stále nabízí prostor pro další studium. Jedna z možností je studium vlivu adsorpce na pásovou strukturu.

7. Bibliography

[1] V. Urbanova, F. Karlicky, A. Matej, F. Sembera, Z. Janousek, J. A. Perman, V. Ranc, K. Cepe, J. Michl, M. Otyepka, and R. Zboril. Fluorinated graphenes as advanced biosensors – effect of fluorine coverage on electron transfer properties and adsorption of biomolecules. *Nanoscale*, **2016**, doi:10.1039/C6NR00353B.

[2] K. S. Novoselov, A. K. Geim, S. V. Morozov, D. Jiang, Y. Zhang, S. V. Dubonos, I. V. Grigorieva, and A. A. Firsov. Electric Field Effect in Atomically Thin Carbon Films. *Science*, 306:666, **2011**, doi:10.1126/science.1102896.

[3] K. S. Novoselov, D. Jiang, F. Schedin, T. J. Booth, V. V. Khotkevich, S. V. Morozov, and A. K. Geim. Two-dimensional atomic crystals. *Proceedings of the National Academy of Sciences of the United States of America*, 102(30):10451–10453, **2005**, doi:10.1073/pnas.0502848102.

[4] E. Starodub, A. Bostwick, L. Moreschini, S. Nie, F. Gabaly, K. McCarty, and E. Rotenberg. In-plane orientation effects on the electronic structure, stability, and Raman scattering of monolayer graphene on Ir(111). *Physical Review B*, 83(12):125428, **2011**, doi:10.1103/PhysRevB.83.125428.

[5] S. Marchini, S. Günther, and J. Wintterlin. Scanning tunneling microscopy of graphene on Ru(0001). *Physical Review B - Condensed Matter and Materials Physics*, 76(7):1–9, **2007**, doi:10.1103/PhysRevB.76.075429.

[6] J. Xue, J. Sanchez-Yamagishi, D. Bulmash, P. Jacquod, A. Deshpande, K. Watanabe, T. Taniguchi, P. Jarillo-Herrero, and B. J. LeRoy. Scanning tunnelling microscopy and spectroscopy of ultra-flat graphene on hexagonal boron nitride. *Nature materials*, 10(4):282–5, **2011**, doi:10.1038/nmat2968.

[7] K. Hermann. Periodic overlayers and moiré patterns: theoretical studies of geometric properties. *Journal of Physics: Condensed Matter*, 24(31):314210, **2012**, doi:10.1088/0953-8984/24/31/314210.

[8] R. R. Nair, A. N. Grigorenko, P. Blake, K. S. Novoselov, T. J. Booth, N. M. R. Peres, T. Stauber, and A. K. Geim. Fine structure constant defines visual transparency of graphene. *Science*, 320(5881):1308, **2008**, doi:10.1126/science.1156965.

[9] K. S. Novoselov, A. K. Geim, S. V. Morozov, D. Jiang, M. I. Katsnelson, I. V. Grigorieva, S. V. Dubonos, and A. A. Firsov. Two-dimensional gas of massless Dirac fermions in graphene. *Nature*, 438(7065):197–200, **2005**, doi:10.1038/nature04233.

[10] C. Kittel. *Introduction to solid state physics*. Wiley, 8. edition, **2005**.

[11] N. Kumar, J. D. Sharma, and P. K. Ahluwalia. First-principle study of nanostructures of functionalized graphene. *Pramana - Journal of Physics*, 82(6):1103–1117, **2014**, doi:10.1007/s12043-014-0758-x.

[12] C. N. R. Rao, A. K. Sood, K. S. Subrahmanyam, and A. Govindaraj. Graphene: The new two-dimensional nanomaterial. *Angewandte Chemie - International Edition*, 48(42):7752–7777, **2009**, doi:10.1002/anie.200901678.

[13] D. W. Boukhvalov and M. I. Katsnelson. Chemical functionalization of graphene. *Journal of Physics: Condensed Matter*, 21(34):344205, **2009**, doi:10.1088/0953-8984/21/34/344205.

[14] V. Singh, D. Joung, L. Zhai, S. Das, S. I. Khondaker, and S. Seal. Graphene based materials: Past, present and future. *Progress in Materials Science*, 56(8):1178–1271, **2011**, doi:10.1016/j.pmatsci.2011.03.003.

[15] C. Mattevi, G. Eda, S. Agnoli, S. Miller, K. A. Mkhoyan, O. Celik, D. Mastrogiovanni, C. Cranozzi, E. Carfunkel, and M. Chhowalla. Evolution of electrical, chemical, and structural properties of transparent and conducting chemically derived craphene thin films. *Advanced Functional Materials*, 19(16):2577–2583, **2009**, doi:10.1002/adfm.200900166.

[16] A. Arramel, A. Castellanos-Gomez, and B. J. van Wees. Band Gap Opening of Graphene by Noncovalent π-π Interaction with Porphyrins. *Graphene*, 02(03):102–108, **2013**, doi:10.4236/graphene.2013.23015.

[17] V. Georgakilas, M. Otyepka, A. B. Bourlinos, V. Chandra, N. Kim, K. C. Kemp, P. Hobza, R. Zboril, and K. S. Kim. Functionalization of graphene: Covalent and non-covalent approaches, derivatives and applications. *Chemical Reviews*, 112(11):6156–6214, **2012**, doi:10.1021/cr3000412.

[18] A. H. Castro Neto, F. Guinea, N. M. R. Peres, K. S. Novoselov, and A. K. Geim. The electronic properties of graphene. *Reviews of Modern Physics*, 81(1):109–162, **2009**, doi:10.1103/RevModPhys.81.109.

[19] M. Dubecky, E. Otyepkova, P. Lazar, F. Karlicky, M. Petr, K. Cepe, P. Banas, R. Zboril, and M. Otyepka. Reactivity of fluorographene: A facile way toward graphene derivatives. *Journal of Physical Chemistry Letters*, 6(8):1430–1434, **2015**, doi:10.1021/acs.jpclett.5b00565.

[20] F. Karlicky, R. Zboril, and M. Otyepka. Band gaps and structural properties of graphene halides and their derivates: A hybrid functional study with localized orbital basis sets. *Journal of Chemical Physics*, 137(3), **2012**, doi:10.1063/1.4736998.

[21] F. Karlicky and M. Otyepka. Band gaps and optical spectra of chlorographene, fluorographene and graphane from G0W0, GW0 and GW calculations on top of PBE and HSE06 orbitals. *Journal of Chemical Theory and Computation*, 9(9):4155–4164, **2013**, doi:10.1021/ct400476r.

[22] F. Karlicky, K. Kumara Ramanatha Datta, M. Otyepka, and R. Zboril. Halogenated graphenes: Rapidly growing family of graphene derivatives. *ACS Nano*, 7(8):6434–6464, **2013**, doi:10.1021/nn4024027.

[23] Y. Sun, Q. Wu, and G. Shi. Graphene based new energy materials. *Energy & Environmental Science*, 4(4):1113, **2011**, doi:10.1039/c0ee00683a.

[24] F. Schwierz. Graphene transistors. *Nature Nanotechnology*, 5(7):487–496, **2010**, doi:10.1038/nnano.2010.89.

[25] M. Pumera. Graphene-based nanomaterials and their electrochemistry. *Chemical Society reviews*, 39(11):4146–57, **2010**, doi:10.1039/c002690p.

[26] S. Ghosh, I. Calizo, D. Teweldebrhan, E. P. Pokatilov, D. L. Nika, A. A. Balandin, W. Bao, F. Miao, and C. N. Lau. Extremely high thermal conductivity of graphene: Prospects for thermal management applications in nanoelectronic circuits. *Applied Physics Letters*, 92(15):2–4, **2008**, doi:10.1063/1.2907977.

[27] G. Tsoukleri, J. Parthenios, K. Papagelis, R. Jalil, A. C. Ferrari, A. K. Geim, K. S. Novoselov, and C. Galiotis. Subjecting a graphene monolayer to tension and compression. *Small*, 5(21):2397–2402, **2009**, doi:10.1002/smll.200900802.

[28] J. H. Lee, Y. K. Choi, H. J. Kim, R. H. Scheicher, and J. H. Cho. Physisorption of DNA nucleobases on h-BN and graphene: VdW-corrected DFT calculations. *Journal of Physical Chemistry C*, 117(26):13435–13441, **2013**, doi:10.1021/jp402403f.

[29] J. Lee, K. A. Min, S. Hong, and G. Kim. Ab initio study of adsorption properties of hazardous organic molecules on graphene: Phenol, phenyl azide, and phenylnitrene. *Chemical Physics Letters*, 618:57–62, **2015**, doi:10.1016/j.cplett.2014.10.064.

[30] R. R. Nair, W. Ren, R. Jalil, I. Riaz, V. G. Kravets, L. Britnell, P. Blake, F. Schedin, A. S. Mayorov, S. Yuan, M. I. Katsnelson, H. Cheng, W. Strupinski, L. G. Bulusheva, A. V. Okotrub, I. V. Grigorieva, A. N. Grigorenko, K. S. Novoselov, and A. K. Geim. Fluorographene: a two-dimensional counterpart of Teflon. *Small*, 6(24):2877–84, **2010**, doi:10.1002/smll.201001555.

[31] K. J. Jeon, Z. Lee, E. Pollak, L. Moreschini, A. Bostwick, C. M. Park, R. Mendelsberg, V. Radmilovic, R. Kostecki, T. J. Richardson, and E. Rotenberg. Fluorographene: A wide bandgap semiconductor with ultraviolet luminescence. *ACS Nano*, 5(2):1042–1046, **2011**, doi:10.1021/nn1025274.

[32] S. Yuan, M. Rösner, A. Schulz, T. O. Wehling, and M. I. Katsnelson. Electronic structures and optical properties of partially and fully fluorinated graphene. *Physical Review Letters*, 114(4):1–5, **2015**, doi:10.1103/PhysRevLett.114.047403.

[33] Z. Wang, S. Qin, C. Wang, and Q. Hui. Fluorine adsorption on the graphene films: From metal to insulator. *Computational Materials Science*, 97:14–19, **2015**, doi:10.1016/j.commatsci.2014.09.018.

[34] M. Pumera, R. Scipioni, H. Iwai, T. Ohno, Y. Miyahara, and M. Boero. A mechanism of adsorption of ??-nicotinamide adenine dinucleotide on graphene sheets: Experiment and theory. *Chemistry - A European Journal*, 15(41):10851–10856, **2009**, doi:10.1002/chem.200900399.

[35] D. Sholl and J. A. Steckel. *Density Functional Theory: A Practical Introduction.* Wiley, **2011**.

[36] W. Koch and M. C. Holthausen. *A Chemist ' s Guide to Density Functional Theory*, volume 3. Wiley-VCH Verlag GmbH, **2001**.

[37] J. P. Perdew, K. Burke, and M. Ernzerhof. Generalized Gradient Approximation Made Simple. *Physical Review Letters*, 77(18):3865–3868, **1996**, doi:10.1103/PhysRevLett.77.3865.

[38] S. Grimme. Semiempirical GGA-type density functional constructed with a long-range dispersion correction. *Journal of Computational Chemistry*, 27(15):1787–1799, **2006**, doi:10.1002/jcc.20495.

[39] J. Klimes, D. R. Bowler, and A. Michaelides. Van der Waals density functionals applied to solids. *Physical Review B - Condensed Matter and Materials Physics*, 83(19), **2011**, doi:10.1103/PhysRevB.83.195131.

[40] P. E. Blöchl. Projector augmented-wave method. *Physical Review B*, 50(24):17953–17979, **1994**, doi:10.1103/PhysRevB.50.17953.